Materials Research

REFERÊNCIA

CAMPOS, Alex Fabiano Cortez et al. Surface charge density cetermination in water based magnetic colloids: a comparative study. **Materials Research**, São Carlos, v. 20, n. 6, p. 1729-1734, nov./dez. 2017. Disponível em: <http://www.scielo.br/scielo.php?script=sci_arttext&pid=S1516-14392017000601729&lng=en&nrm=iso>. Acesso em: 18 jan. 2018. Epub Oct 09, 2017. doi: http://dx.doi.org/10.1590/1980-5373-mr-2017-0649.

Surface Charge Density Determination in Water Based Magnetic Colloids: a Comparative Study

Alex Fabiano Cortez Campos[a,b]*, Webert Costa de Medeiros[a], Renata Aquino[a,b], Jerome Depeyrot[b]

[a]*Laboratório de Nanociência Ambiental e Aplicada, Universidade de Brasília, Planaltina, DF, Brazil*
[b]*Laboratório 3NANO, Instituto de Física, Universidade de Brasília, Brasília, DF, Brazil*

This work focuses on the systematic investigation of the two well-established methods of structural surface charge density determination on magnetic colloids, labeled as Single Potentiometric Method (SPM) and Potentiometric-Conductometric Method (PCM). To compare some important features of the methods we determined the structural surface charge density of magnetic colloids samples based on $CoFe_2O_4@\gamma\text{-}Fe_2O_3$ core-shell nanoparticles with three different mean sizes using both strategies. Concerning quickness, easiness and cost, the PCM has proved to be more advantageous than the SPM. Regarding the effectiveness, both methods were consistent in determining the saturation value of the structural charge, but the SPM was more accurate to describe the pH-dependence of the concentration of the charged surface sites. Considering the chemical safety, the methods are equivalent. Finally, both the SPM and PCM are reproducible and can be effectively applied to determine the saturation value of the surface charge density on magnetic colloids.

Keywords: surface charge density, magnetic colloids, nanoparticles, electrochemical methods.

1. Introduction

Magnetic nanocomposites have been attracting great attention owing to their unique physicochemical properties. These materials have been widely used in many different fields, especially in nanobiotechnology[1,2]. Among their properties, the surface charge density plays a key role not only in colloidal stability, but also in many applications such as cellular uptake[3,4], drug delivery[5], biosensing[6,7] and removal of pollutants from wastewater[8]. In water dispersions of magnetic nanoparticles based on metal oxides, the nanoparticle surface presents an amphoteric behavior and becomes charged from protonation/ deprotonation reactions according to[9]:

$$\equiv MOH + H_3O^+ \equiv MOH_2^+ + H_2O \quad (1)$$

$$\equiv MOH + OH^- \equiv MO^- + H_2O, \quad (2)$$
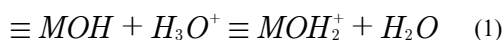
where M is the metal on surface. In absence of specific adsorbing ions, the nanoparticle surface has a characteristic point of zero charge (PZC), which is the pH where the concentration of positively and negatively sites are in equal amount. At pH < PZC the surface is positively charged while at pH > PZC it develops negative charge. Moreover, for *p*H ≤ 3 and *p*H ≥ 11, the particle surface is charge saturated since the number of charged surface sites is no more varying[10,11]. In this context, the structural surface charge density (σ_0) can be calculated using the equation:

$$\sigma_0 = \frac{FV}{A_T}([\equiv MO_2^+] - [\equiv MO^-]) , \quad (3)$$

where F is the Faraday constant and V the volume of colloid dispersion. $[\equiv MOH_2^+]$ and $[\equiv MO^-]$ are the concentration of charged surface sites. A_T is the total surface area of nanoparticles, which can be evaluated from X-rays diffraction or transmission electronic microscopy measurements taking into account the polydispersity in size and the volume fraction of the sample. Otherwise, A_T can be related to the specific surface area of the solid determined from BET analysis[12].

Besides the pH of the medium, the ionic strength of the dispersion can have a direct influence on the nanoparticles surface charge density. In fact, the presence of specific ions at the solid-liquid interface can induce the formation of chemical bonds where the ions bind the surface sites through covalent interactions in addition to the pure Coulombic contributions[13]. The presence of non-specific ions is indifferent to the surface charge, therefore they are commonly used as background electrolyte to monitor the ionic strength of the medium.

In the case of diluted water based magnetic nanocolloids, the current literature provides two different experimental strategies to determine the nanoparticle structural surface charge density, both based on potentiometric acid-base titrations. In this paper, for convenient purposes, we will call them Single Potentiometric Method (SPM) and Potentiometric-Conductometric Method (PCM).

*e-mail: relex@unb.br

In the SPM[14,15] the pH of the magnetic colloid sample is adjusted to the PZC inducing rapid coagulation. Then, the coagulated nanoparticles are washed thoroughly with distilled water to ensure the particles are uncharged and the solvent is free of ions. Next, aliquots of standard solutions of acid or base, usually HNO_3 or NaOH, are added to the precipitate in order to titrate the acidic or basic range. The amounts of the surface protonated $n_{\equiv MOH_2^+}$ and deprotonated $n_{\equiv MO^-}$ sites (mol) is deduced by measuring potentiometrically the pH of the resulting mixture since it corresponds to the difference between the number of added H^+/OH^- ions and the number of H^+/OH^- remaining in the dispersion, according to equations:

$$n_{\equiv MOH_2^+} = n_{H^+}^{add} - n_{H^+}^{free} - n_{H^+}^{w}; \text{ and} \qquad (4)$$

$$n_{\equiv MO^-} = n_{OH^-}^{add} - n_{OH^-}^{free} - n_{OH^-}^{w}, \qquad (5)$$

where $n_{H^+}^{add}$ and $n_{OH^-}^{add}$ are, respectively, the number of moles of protons and hydroxide ions dropped by the titrant, $n_{H^+}^{free}$ and $n_{OH^-}^{free}$ are the protons and hydroxide ions that remain free in dispersion after the titrant addition and $n_{H^+}^{w}$ and $n_{OH^-}^{w}$ are the protons and hydroxide ions neutralized in the self-ionization of the water.

In another strategy, PCM[10,16], the titrations of the magnetic colloid samples start from acidic (pH ≤ 3) or alkaline (pH ≥ 11) medium, when simultaneous potentiometric and conductometric readings are carried out. The single potentiometric curve does not allow the evaluation of the equivalence points since it does not present sharp breaks. In this way, the equivalence points are determined from the conductometric curve, which present abrupt changes of slope. Thus, it is possible to determine the total concentration of the surface sites C_T using the mass balance and the volume of titrant reagent used to titrate the nanoparticle surface. The pH-dependence of the surface charge density is achieved from a Two-pK Model according to:

$$\sigma_0(pH) = \frac{F}{A_T} V \left(\frac{10^{-2\,pH} - 10^{-(pK_1 + pK_2)}}{10^{-2pH} + 10^{-(pH + pK_1)} + 10^{-(pK_1 + pK_2)}} \right) C_T, \quad (6)$$

where pK_1 and pK_2 corresponds to the thermodynamical constants ($pK = -logK$) related to the protonation/deprotonation mechanism. These constants are determined from the Henderson-Hasselbalch equation using the potentiometric data. It is worth to comment that $C_T \approx [\equiv MOH_2^+]$ in strong acidic medium while $C_T \approx [\equiv MO^-]$ in strong alkaline medium.

The surface charge density in water based magnetic colloids strongly depends on the nanoparticle mean size. It has been evidenced that the surface charge for smaller particles decreases drastically because of the spatial confinement at nanoscale[10]. This behavior is related to surface sites with very low acidity and unusual coordination environment combined with a quantum size effect, which affects charge generation.

In this context, the aim of the present paper is to investigate these two methods of surface charge determination in terms of their main features, including their advantages and disadvantages. Parameters such as quickness, easiness, cost, effectiveness and chemical safety were considered in order to compare their general characteristics. Moreover, taken in conjunction with the laboratory resources, these parameters might influence the decision about the choice of method for surface charge density determination on magnetic colloids. The first part of the paper presents the used materials and methods. A brief description of the chemical synthesis is provided, followed by chemical analysis results to check the chemical composition of our synthesized nanoparticles. Since the surface charge depends on the nanoparticles mean size, magnetic nanocolloids samples based on particles of three different diameters were prepared to investigate if the size affects the methods' parameters. Next, the structure and mean size of the nanoparticles are characterized from X-ray diffraction measurements. Furthermore, the experimental procedure of the SPM and the PCM is described. Then, the results of all experiments are presented. Finally, the general features of the two different strategies to determine the structural surface charge density on magnetic colloids are discussed in terms of the above-mentioned parameters.

2. Experimental

2.1 Reagents

The following pro analyse (P.A.) grade reagents, supplied from Vetec Química Fina, were used for nanoparticles synthesis: $FeCl_3 \cdot 6H_2O$ (purity 99%), $Fe(NO_3)_3 \cdot 9H_2O$ (purity 99%), $Co(NO_3)_2 \cdot 6H_2O$ (purity 98%), $MnCl_2 \cdot 4H_2O$ (purity 98%), NaOH (purity 99%), $NaNO_3$ (purity 99%) and HNO_3 (63% in water). The aqueous solutions were prepared with deionized water Type I (Millipore Milli-Q. Gradient quality).

2.2 Sample synthesis

The preparation of the magnetic nanocolloid precursor samples was carried out by following the procedures described elsewhere[17,18]. Firstly, $CoFe_2O_4$ nanoparticles were synthesized using a hydrothermal coprecipitation of aqueous solutions of $Co(NO_3)_2$ and $FeCl_3$ in a strong alkaline medium (NaOH). By changing both the hydroxide concentration of the synthesis medium[19] and the speed of reagents addition[20] it has been possible to control the nanoparticles diameter in order to obtain samples with three different mean sizes. The dispersion of the $CoFe_2O_4$ nanoparticles in aqueous acid medium leads to no viable nanocolloids because this kind of nanoparticles tend to slowly dissolve in those conditions[17]. Thus, after the coprecipitation, the precipitate was washed with distilled water several times and it was hydrothermally treated with a solution of $Fe(NO_3)_3$ 0.5 mol L^{-1}. This treatment creates a layer of maghemite (γ-Fe_2O_3) around the precursor

particles that avoid their dissolution in acid medium. Finally, the particles were conveniently peptized in an acidic medium (pH ≈ 2) by adjustment of pH and ionic strength, resulting in a stable sol of high quality. It is worth to mention that the phenomenon of nanoparticles dissolution in acidic medium also takes place for other ferrite-based nanoparticles (MFe_2O_4; M = Mn, Ni, Cu Zn) used in ferrofluids elaboration and the same surface treatment must be performed to obtain magnetic nanocolloids with long-term stability.

2.3 Chemical composition of the nanoparticles

The hydrothermal surface treatment with $Fe(NO_3)_3$ induces a superficial iron enrichment of the nanoparticles, therefore their composition can be expressed using a core-shell model, where the nanoparticles are made of the ferrite core ($CoFe_2O_4$) surrounded by a superficial layer of maghemite ($CoFe_2O_4@\gamma\text{-}Fe_2O_3$) whose structure has been extensively studied in reference 20. The volume fraction of nanoparticles in the prepared nanocolloid ϕ_P was determined according to this model: the volume fraction of the core is proportional to the concentration of cobalt (II) ions $[Co^{2+}]$ and the volume fraction of the shell is proportional to the iron concentration of the shell equal to $0.5([Fe^{3+}] - 2 [Co^{2+}])$, $[Fe^{3+}]$ being the total iron concentration. The concentration of metallic cations was measured by flame atomic absorption spectroscopy. The samples investigated in this work present a volume fraction of particles around 1%, where the nanocolloidal dispersion can be considered as a gas of isolated particles[21].

2.4 Structure and size of nanoparticles

The characterization of the crystalline structure of our magnetic nanoparticles has been achieved from X-rays diffraction measurements performed on powder samples obtained after evaporation of the liquid carrier at the Brazilian Synchrotron source (Laboratório Nacional de Luz Síncrotron - LNLS). It was used the D12A-XRD1 beamline, monochromatized at 6.01 keV (λ = 2.063 Å) and the diffraction patterns were obtained typically within 20° ≤ 2θ ≤ 80° interval, with 0.04° step and 10 s counting time. The mean size of the nanoparticles (d_{XR}) was calculated using the Scherrer equation.

2.5 Titrations procedures

In this work, all titrations were performed in triplicate considering 40 mL of the magnetic colloid sample (volume fraction ϕ_P = 0.4%), under CO_2-free atmosphere and using $NaNO_3$ 0.01 mol L^{-1} as background indifferent electrolyte to keep a constant ionic strength. Before any titration, alkaline reagents were stirred and degassed by purified nitrogen during 10 minutes to avoid carbonation phenomena. In order to keep an efficient homogenization in all pH range, the dispersion was vigorously stirred in the course of titration. The titrants solutions were duly standardized.

The titrations were done with an electronic burette Optilab. The potentiometric readings were performed with a pHmeter Quimis Q400AS using a pH glass double-junction electrode while the conductivity was measured with a conductometer Quimis Q405M using a conductivity cell specially designed for colloidal dispersions. The direct measurement of the pH was achieved after the calibration of the electrode in the acidic and alkaline pH ranges, using standard buffers of pH equal to 4, 7 and 9, respectively. The electrical conductivity κ was determined indirectly by measuring the corresponding conductance of the nanocolloid dispersion. The cell constant was obtained by measuring the conductivity of a standard solution of potassium chloride (KCl) 3 mol L^{-1} of known conductivity.

In order to apply the SPM, the pH of the sample was adjusted to the PZC by addition of standard solution of sodium hydroxide (NaOH) 0.1 mol L^{-1}. After the coagulation of the particles (pH ≈ 7.1), the precipitated was washed three times with deionized water to remove the free ions of the medium. Next, the sample was titrated by using standard solution of nitric acid (HNO_3) 0.1 mol L^{-1} until pH ≈ 2. For another aliquot of the magnetic colloid, the same procedure of PZC adjustment was repeated and then the sample was titrated with standard solution of sodium hydroxide 0.1 mol L^{-1} until pH ≈ 12 to cover the alkaline range. The titrations were limited to 2 < pH < 12, because for extreme pH conditions the accuracy on the determination of the number of protonated/deprotonated sites is poor since the amount of free H^+/OH^- ions in the dispersion becomes large compared to the amount of H^+ bounded/released on particle surface[9]. In the case of the PCM, it was not employed any pH adjustment procedure. The aliquot of the acid magnetic sample was titrated from pH ≈ 2 to pH ≈ 12 with standard solution of sodium hydroxide 0.1 mol L^{-1} measuring simultaneously the pH and the conductivity of the medium.

3. Results and Discussion

Figure 1 shows a typical X-rays diffractogram of the nanoparticles (sample A) which exhibits several lines corresponding to the characteristic interplanar spacings (220), (311), (400), (422), (511) and (440) of the spinel structure. The size of the cubic cell was found equal to 0.832 nm to be compared with the ASTM value equal to 0.833 nm for $CoFe_2O_4$ bulk material. The mean crystal size was deduced equal to 13.8 nm by means of the Scherrer formula, using the width at half-maximum of the most intense diffraction line (311). For the other samples investigated in this work, the value of the nanoparticle mean sizes is reported in Table 1.

Figure 2 depicts the two typical independent titration curves obtained using the SPM (sample A). The results were presented in a single curve, where negative values of titrant volume refer to the titration of the acid range while positive
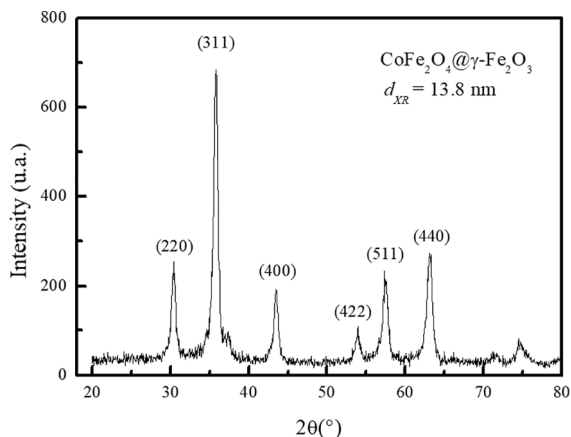
Figure 1. XRD pattern for sample A where the characteristic (hkl) interplanar planes of the spinel structure are labeled.

Table 1. Value of nanoparticles mean sizes (d_{XR}) and results of the saturation value of the surface charge density (σ_0^{sat}) obtained with the two methods for all samples investigated

Sample	d_{XR}(nm)	σ_0^{sat}(C m^{-2}) (SPM)	σ_0^{sat}(C m^{-2}) (PCM)
A	13.8	0.31 ± 0.01	0.32 ± 0.01
B	8.8	0.24 ± 0.01	0.26 ± 0.01
C	5.9	0.21 ± 0.01	0.22 ± 0.01

values are related to the titration of the alkaline range. As it can be seen, the titrant volume used to titrate the magnetic colloid sample was almost the same in both pH regions. It indicates that, in these experimental conditions, the surface charge can be considered symmetrical with respect to the PZC as already observed in similar systems[7]. From the titration data and using the equations (4) and (5) the number of moles of surface protonated/deprotonated sites was found equal to 0.23 mmol. The inset of figure 2 clearly shows that the number of charged surface sites tends to a saturation value (σ_0^{sat}), which corresponds to 0.31 ± 0.01 C m^{-2} for the sample A. As previously reported[10,12] this maximum value of the surface charge density depends on the structure, composition and mean size of the nanoparticles.

Figure 3 presents the typical titration curves of the samples using the PCM (sample A), where the equivalence points EP$_1$ and EP$_3$ were determined by the graphical method[22] and delimit three distinct regions. The first one corresponds to the neutralization of free protons of the bulk solution. After EP$_3$, the third region is related to the excess of alkaline reagent. The second region, between EP$_1$ and EP$_3$, corresponds to the titration of particle surface, i.e., the neutralization of the protons released from the active surface sites. There is a second equivalence point EP$_2$ between EP$_1$ and EP$_3$, which is calculated by the semi-sum of EP$_1$ and EP$_3$, since the volume of titrant must be equal to neutralize each proton of the nanoparticle surface. Using the determined equivalence points and the mass balance, the total concentration of the
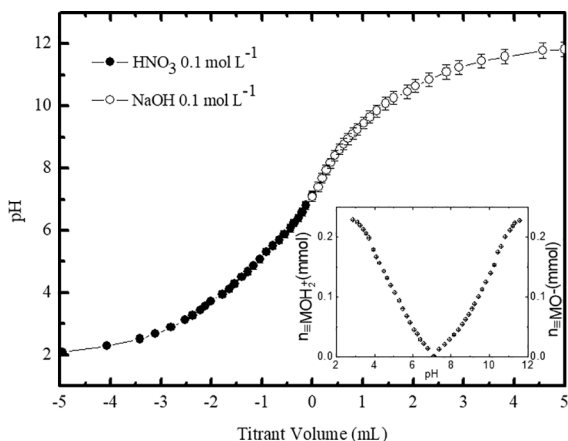

Figure 2. Typical curves of potentiometric titrations starting from the PZC (sample A). Negative values of titrant volume refer to the titration of the acid range while positive values are related to the titration of the alkaline range. The inset shows the number of moles of surface protonated (left) and deprotonated (right) in function of pH.

surface sites was calculated leading to a saturation value of the surface charge density equal to 0.32 ± 0.01 C m^{-2}. The pK values were found equal to pK_1 = 5.0 and pK_2 = 9.5 in very good agreement with other determinations in similar systems[23].
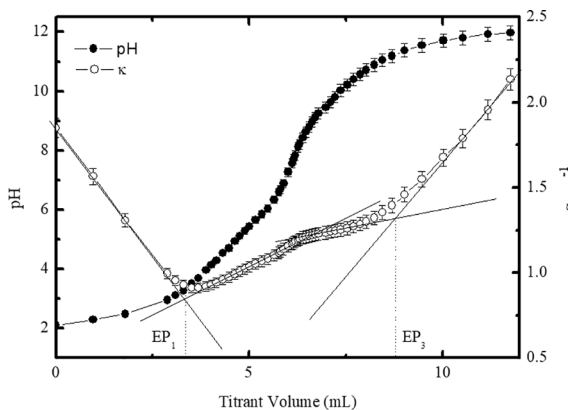

Figure 3. Typical curves of simultaneous potentiometric-conductometric titrations (sample A). The equivalence points are determined by using the graphical method.

Figure 4 exhibits the typical pH-dependence of the surface charge density determined with both methods (sample A). The curve related to the SPM was evaluated from equations 3, 4 and 5 while that of the PCM was obtained from equation 6.

With respect to quickness, the PCM is more advantageous than the SPM. In fact, using the latter it is necessary to perform two titrations for the same sample: one for the acidic range and other for the basic range. In addition, the procedure of precipitate washing and pH adjustment demand approximately 20-30 minutes. With the PCM, the sample is titrated from its initial pH, which can be acidic or basic, depending on the type of magnetic colloid. In this method,
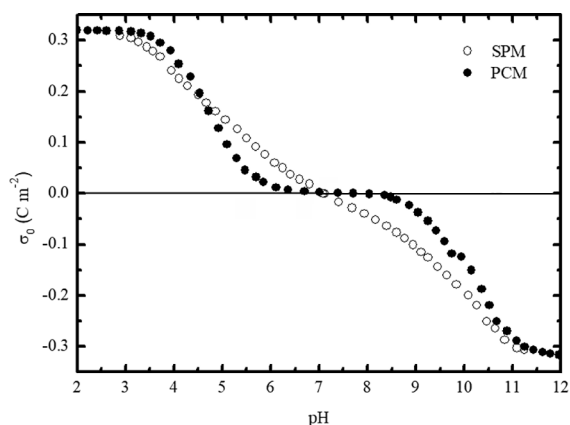
Figure 4. Typical pH-dependence of the surface charge density determined with both methods (sample A).

the additional collection of conductivity data has no influence on the total time of analysis because it is simultaneously measured with pH and requires no additional time for reading in the equipment.

Regarding the easiness of the methods, the PCM also takes advantage compared to the SPM. Once more, one must consider the procedure of pH adjustment to PZC. Regardless of time, this procedure is laborious because after nanoparticles coagulation it is necessary to wash the precipitate with deionized water many times to remove the excess of free ions in solution. Since the supernatant is removed by suction, the process must be carried out carefully to avoid the loss of nanoparticles. In addition, the aggregates formed at PZC may decrease the total surface area leading to uncertainty on the determination of the surface charge density. This is not observed with the PCM because in this method, the titration starts from pH values where the samples are stable sols and the dispersions are kept under vigorous stirring, reducing the possibility of aggregate formation.

In order to compare the cost of analysis, it is necessary to point out important features of both methods. While the SPM involves only the potentiometric titrations, in the PCM potentiometric and conductometric measurements are simultaneously carried out, leading to an additional cost of equipment (conductometer, conductometric cell and the respective temperature sensor). However, the SPM uses twice as much volume of colloid as the PCM, since it requires two aliquots from each sample to titrate the acidic and the alkaline ranges. Considering the experimental difficulty to elaborate stable magnetic colloid samples and the cost of reagents used during the synthesis, it appears that even with the additional cost of purchasing the equipment, the PCM is more cost effective than the SPM.

Regardless of technical issues, the most important parameter to be considered in this investigation is the effectiveness of the methods, i.e. their ability to provide reliable results

in agreement with the literature. In this way, according to table 1, the saturation value of the surface charge density determined with the two methods show excellent agreement with each other and they are consistent with previous determinations in similar magnetic colloids[10,14,15,24] proving that both are effective. Nevertheless, the methods exhibit a significant different profile of the pH dependence of the surface charge density as shown in figure 4. With the PCM, the characteristic evolution of the surface charge with the pH arises from the theoretical speciation of the charged sites, according to the Two-pK Model (eq. 6), which considers the charged surface sites being equivalent and independent. Thus, the pH-dependence of the surface charge density is best described by the SPM.

Finally, concerning the chemical safety both methods are equivalent, since they use the same reagents and generate the same chemical wastes not only in the steps of magnetic colloid elaboration but also in the titrimetric procedures.

4. Conclusions

In this work, a comparative study of the two well-established methods of surface charge density determination on magnetic colloids was conducted. Samples based on core-shell $CoFe_2O_4@\gamma\text{-}Fe_2O_3$ nanoparticles with three different mean sizes were used. These core-shell type nanoparticles have a great potential to be applied as precursors of biocompatible magnetic fluids and as magnetic nanoadsorbents for wastewater remediation. Important characteristic parameters of the methods were considered, such as quickness, easiness, cost, effectiveness and chemical safety. Concerning the three first parameters, the PCM has proved to be more advantageous than the SPM, since it demands less time of analysis, involves simple technical procedures and requires less amount of reagents, supplies and samples. The results of the saturation value of the surface charge determined with the two methods were found in very good agreement indicating that both are effective regardless the nanoparticles mean size. However, with respect to the pH dependence of the surface charge density, the methods exhibited important discrepancies. The SPM is more accurate to describe the variation of the concentration of the charged surface sites with the pH because it does not depend on the Two-pK model. The chemical safety of the two methods are equivalent. In conclusion, both the SPM and PCM are reproducible and can be effectively applied to determine the saturation value of the surface charge density on magnetic colloids.

5. Acknowledgements

6. References

1. Lai W, Wei Q, Xu M, Zhuang J, Tang D. Enzyme-controlled dissolution of MnO_2 nanoflakes with enzyme cascade amplification for colorimetric immunoassay. *Biosensors and Bioelectronics*. 2017;89(Pt 1):645-651.

2. Tang D, Su B, Tang J, Ren J, Chen G. Nanoparticle-Based Sandwich Electrochemical Immunoassay for Carbohydrate Antigen 125 with Signal Enhancement Using Enzyme-Coated Nanometer-Sized Enzyme-Doped Silica Beads. *Analytical Chemistry*. 2010;82(4):1527-1534.

3. Osaka T, Nakanishi T, Shanmugam S, Takahama S, Zhang H. Effect of surface charge of magnetite nanoparticles on their internalization into breast cancer and umbilical vein endothelial cells. *Colloids and Surfaces B-Biointerfaces*. 2009;71(2):325-330.

4. Calatayud MP, Sanz B, Raffa V, Riggio C, Ibarra MR, Goya GF. The effect of surface charge of functionalized Fe_3O_4 nanoparticles on protein adsorption and cell uptake. *Biomaterials*. 2014;35(24):6389-6399.

5. McBain SC, Yiu HHP, Dobson J. Magnetic nanoparticles for gene and drug delivery. *International Journal of Nanomedicine*. 2008;3(2):169-180.

6. Lin Y, Zhou Q, Li J, Shu J, Qiu Z, Lin Y, et al. Magnetic Graphene Nanosheet-Based Microfluidic Device for Homogeneous Real-Time Electronic Monitoring of Pyrophosphatase Activity Using Enzymatic Hydrolysate-Induced Release of Copper Ion. *Analytical Chemistry*. 2016;88(1):1030-1038.

7. Lin Y, Zhou Q, Tang D, Niessner R, Knopp D. Signal-On Photoelectrochemical Immunoassay for Aflatoxin B1 Based on Enzymatic Product-Etching MnO_2 Nanosheets for Dissociation of Carbon Dots. *Analytical Chemistry*. 2017;89(10):5637-5645.

8. Wang P, Lo IMC. Synthesis of mesoporous magnetic $\gamma\text{-}Fe_2O_3$ and its application to Cr(VI) removal from contaminated water. *Water Research*. 2009;43(15):3727-3734.

9. Illés E, Tombácz E. The effect of humic acid adsorption on pH-dependent surface charging and aggregation of magnetite nanoparticles. *Journal of Colloid and Interface Science*. 2006;295(1):115-123.

10. Campos AFC, Aquino R, Tourinho FA, Paula FL, Depeyrot J. Influence of the spatial confinement at nanoscale on the structural surface charging in magnetic nanocolloids. *The European Physical Journal E*. 2013;36(4):9856.

11. Costo R, Bello V, Robic C, Port M, Marco JF, Morales MP, et al. Ultrasmall Iron Oxide Nanoparticles for Biomedical Applications: Improving the Colloidal and Magnetic Properties. *Langmuir*. 2012;28(1):178-185.

12. Schreier M, Feltes TE, Schaal MT, Regalbuto JR. The determination of oxide surface charging parameters for a predictive metal adsorption model. *Journal of Colloid and Interface Science*. 2010;348(2):571-578.

13. Tombácz E. pH-dependent surface charging of metal oxides. *Periodica Polytechnica-Chemical Engineering*. 2009;53(2):77-86.

14. Lucas IT, Durand-Vidal S, Dubois E, Chevalet J, Turq P. Surface Charge Density of Maghemite Nanoparticles: Role of Electrostatics in the Proton Exchange. *Journal of Physical Chemistry C*. 2007;111(50):18568-18576.

15. Lucas IT, Durand-Vidal S, Bernard O, Dahirel V, Dubois E, Dufrêche JF, et al. Influence of the volume fraction on the electrokinetic properties of maghemite nanoparticles in suspension. *Molecular Physics*. 2014;112(9-10):1463-1471.

16. Campos AFC, Tourinho FA, da Silva GJ, Lara M, Depeyrot J. Nanoparticles superficial density of charge in electric double-layered magnetic fluid: A conductimetric and potentiometric approach. *TheEuropean Physical Journal E*. 2001;6(1):29-35.

17. Tourinho FA, Franck R, Massart R. Aqueous ferrofluids based on manganese and cobalt ferrites. *Journal of Materials Science*. 1990;25(7):3249-3254.

18. Sousa MH, Tourinho FA, Depeyrot J, Silva GJ, Lara MCFL. New Electric Double-Layered Magnetic Fluids Based on Copper, Nickel, and Zinc Ferrite Nanostructures. *Journal of Physical Chemistry B*. 2001;105(6):1168-1175.

19. Aquino R, Tourinho FA, Itri R, Lara MCFL, Depeyrot J. Size control of $MnFe_2O_4$ nanoparticles in electric double layered magnetic fluid synthesis. *Journal of Magnetism and Magnetic Materials*. 2002;252:23-25.

20. Gomes JA, Sousa MH, Tourinho FA, Aquino R, da Silva GJ, Depeyrot J, et al. Synthesis of Core-Shell Ferrite Nanoparticles for Ferrofluids: Chemical and Magnetic Analysis. *Journal of Physical Chemistry C*. 2008;112(16):6220-6227.

21. Mériguet G, Cousin F, Dubois E, Boué F, Cebers A, Farago B, et al. What tunes the structural anisotropy of magnetic fluids under a magnetic field? *Journal of Physical Chemistry B*. 2006;110(9):4378-4386.

22. Chromiak E. Computer-program for examination of acids by conductimetric potentiometric titration. *Analyst*. 1995;120(1):149-153.

23. Campos AFC, Tourinho FA, Aquino R, Depeyrot J. Probing interface and finite size effects in magnetic ferrite nanoparticles by electrochemical measurements. *Journal of Magnetism and Magnetic Materials*. 2007;310(2 Pt 3):2847-2849.

24. Lucas IT, Dubois E, Chevalet J, Durand-Vidal S. Reactivity of nanocolloidal particles gamma-Fe_2O_3 at the charged interfaces - Part 1. The approach of particles to an electrode. *Physical Chemistry Chemical Physics*. 2008;10(22):3263-3273.